

# Los Alamos

NATIONAL LABORATORY

## memorandum

Spallation Neutron Source Project Office

To/MS: Distribution  
 From/MS: Sergey Kurennoy / H824  
 Phone/FAX: 5-1459 / 5-9998  
 Email: kurennoy@lanl.gov  
 Symbol: SNS: 00-54  
 Date: July 26, 2000

**SUBJECT:** Beam position monitors for DTL in SNS linac

**Copies to:**

SNS File	MS H824		
J.H. Billen	MS H824 (e-copy)	R.E. Shafer	MS H808 (e-copy)
J.D. Gilpatrick	MS H808 (e-copy)	J.E. Stovall	MS H824 (e-copy)
R.A. Hardekopf	MS H824 (e-copy)	A.V. Aleksandrov	ORNL (e-copy)
A.J. Jason	MS H808 (e-copy)	P.R. Cameron	BNL (e-copy)
R.B. Miller	MS H824 (e-copy)	L.R. Doolittle	LBNL (e-copy)
J.F. O'Hara	MS H808 (e-copy)	J.D. Galambos	ORNL (e-copy)
J.F. Power	MS H824 (e-copy)	T.J. Shea	ORNL (e-copy)

***Abstract.** Electromagnetic modeling of beam positions monitors (BPMs) for the drift-tube linac (DTL) section of the SNS linac has been performed to choose an optimal design and calculate the signal power on the BPM electrodes due to the RF field in the DTL. Results are presented and discussed.*

### 1. Introduction

Beam position monitors (BPMs) provide information about the transverse position of the beam, which is used to steer the beam properly in a linac with steering magnets. In addition, the BPMs in the SNS linac will also serve as the beam phase detectors, see [1]. The BPM in the coupled-cavity linac (CCL) section of the SNS linac will have four 60-degree stripline electrodes shorted at one end [1]. The design of the CCL BPMs was optimized using electromagnetic modeling with MAFIA [2] to maximize the beam signal for a given electrode length and provide a good linearity.

Typically, in DTL structures there is no room for the BPMs and/or steerers. However, the SNS DTL will have every third drift tube (DT) empty, and there is an option to place there BPM pickups and steering magnets to provide a better quality beam at the DTL output. These BPMs have to fit inside the drift tubes, and that leads to certain restrictions and requirements to their design. In addition to obvious geometrical constraints, a BPM pickup inside of a drift tube is placed very close to the accelerating RF field that can induce a strong signal at the RF frequency. For the CCL structure, where the BPMs are located in the relatively long drifts between the RF cavities, this problem is not so important. Moreover, for the SNS linac, the CCL RF frequency

805 MHz is twice the bunch repetition frequency,  $f_b=402.5$  MHz, while in the DTL the RF frequency is equal to 402.5 MHz.

To study the feasibility of BPMs in the SNS DTL, we use the electromagnetic (EM) code package MAFIA [2]. First, the 4-electrode BPMs for the CCL are scaled down to fit inside the drift tubes, using electrostatic computations to adjust the BPM cross-section dimensions to provide 50- $\Omega$  transmission lines. After that we apply time-domain 3-D simulations with an SNS beam microbunch passing through the BPM pickup along the chamber axis to calculate the beam-induced signal power on the electrodes, in particular, for the first and second harmonics of the SNS bunch repetition frequency  $f_b=402.5$  MHz. Finally, we compute the RF-induced signal power on the BPM electrodes, and optimize the pickup position inside the drift tube to minimize this power.

## 2. Design and electromagnetic modeling of DTL BPMs

To conform the geometrical restrictions of placing the BPM pickup inside of DTs, we look at the tightest spot – the third DT in the second tank of the DTL (there will be no BPMs in the first tank). The length of this DT along the beam is about 8 cm, and the beam-pipe inner radius in the DT is 12.5 mm. A part of the longitudinal cross section of this DT is shown in a SUPERFISH picture in Fig. 1.

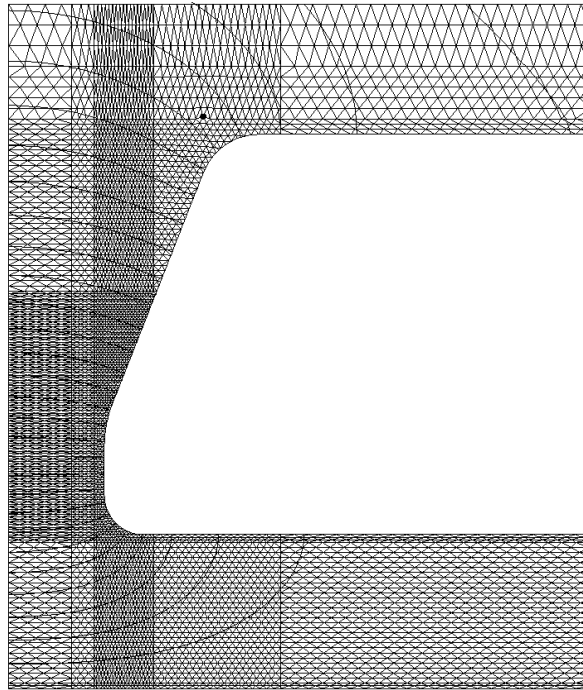


**Figure 1:** SUPERFISH mesh around the DT for a near-axis part of the DTL half-cell radial cross section for SNS linac (courtesy of James H. Billen). The electric field lines for the accelerating mode at 402.5 MHz are shown. The lower boundary is the chamber axis; z-axis cut is about 4.8 cm.

We are going to use the same 4-electrode BPM design with one-end-shortened stripline electrodes that was developed for the CCL BPMs [1]. This design provides a rigid and robust mechanical structure. It is bi-directional and has only four connectors, all on one end of the BPM, which can be very important for mounting the device inside of DTs. The optimized CCL BPMs have an excellent linearity. The MAFIA model of the CCL BPM assembly consisting of a box with 4 electrodes on a beam pipe is shown in Fig. 2. The electrodes are flush with the beam pipe, shorted at one end, and have 50- $\Omega$  connectors on the other end. For the DTL, the beam pipe radius is 12.5 mm, and we reduce the electrode length along the beam to 32 mm (instead of 40 mm in CCL). The electrode subtended angle remains 60°. The 50- $\Omega$  terminations of the electrodes are modeled by filaments with discrete elements, 50- $\Omega$  resistors in this case.

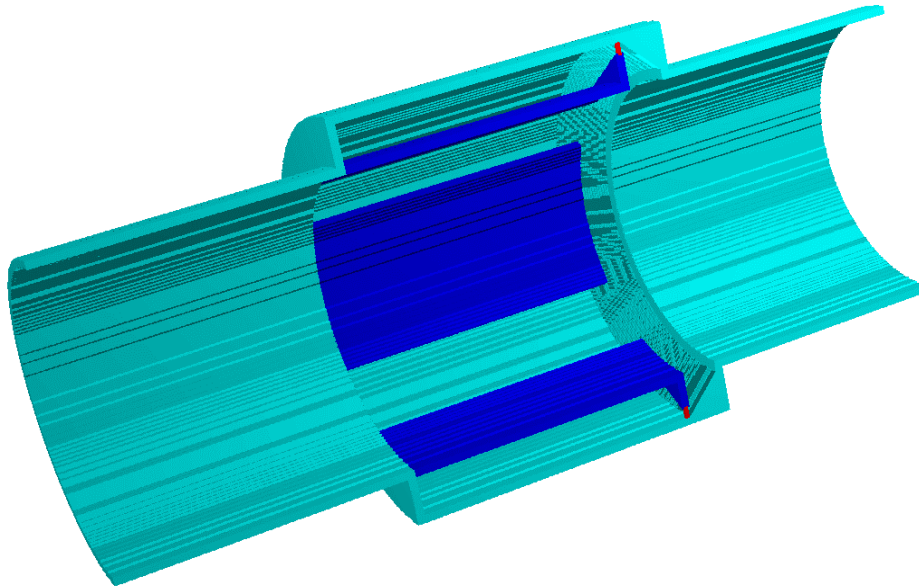


**Figure 2:** MAFIA model of CCL BPMs (one-half cutout) with cone-tapered box and electrodes (dark-blue) with tapered terminations (connectors are shown in red).

First, in a static approximation we solve a 2-D electrostatic problem to find the potential distribution in the cross section for a given potential on an active electrode, to adjust the BPM cross section dimensions for the electrodes to form 50- $\Omega$  transmission lines. As a result, the inner radius of the BPM enclosure comes out to be 17 mm, for the electrode thickness of 1 mm. The circular gap near connectors has a width of 4 mm, and the cone tapering has a 45° slope. The length of transitions from the electrodes to the 50- $\Omega$  coaxial connectors is increased to 4 mm in the direction along the chamber axis, compared to the model of Fig. 2 with only 1 mm, to simplify the connections. The resulting model of the DTL BPM placed inside of a simplified drift tube is shown in Fig. 3. We restrict ourselves here with a rough cylindrical approximation for the DT, without the sloped faces and smooth edges like in Fig. 1. This approximation will be sufficient, however, to estimate the signal power induced by the RF field on the BPM electrodes. The real DT, in addition to having an optimized shape for the higher shunt impedance, is also hollow inside. The inner space can be used to place connectors and cables, which will come out of the DTL tank through the stem supporting the DT.

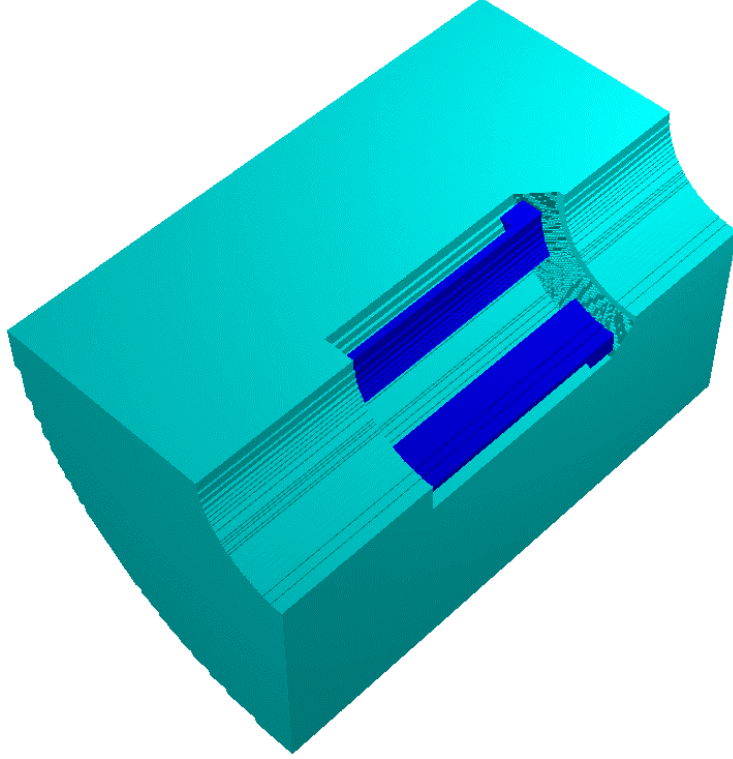


**Figure 3:** MAFIA model of BPM inside of DT (one quarter). Halves of two electrodes (dark-blue) with tapered terminations are placed in the middle of DT. Connectors are not displayed.

### **A. Beam-induced signal in DTL BPM**

We proceed with direct 3D time-domain computations using an ultra relativistic ( $\beta=1$ ) bunch passing the structure at the axis or parallel to the axis. A Gaussian longitudinal charge distribution of the bunch with the total charge  $Q=0.14$  nC and the rms length  $\sigma=5$  mm, corresponding to the 56-mA current in the baseline SNS regime with 2-MW beam power at 60 Hz, was used in the simulations. Unfortunately, the MAFIA time-domain code T3 at present cannot simulate the open boundary conditions on the beam pipe ends for non ultra relativistic ( $\beta<1$ ) beams. Similar to Ref. [1], the ultra relativistic MAFIA results are used to fix parameters of an analytical model for the BPMs at  $\beta=1$ , and then to extrapolate results to  $\beta<1$  analytically. For illustration, the voltage on the BPM electrodes versus time for the case of a  $\beta=1$  beam passing on the chamber axis is shown in Fig. 4a, and its Fourier transform in Fig. 4b. The Fourier spectrum of the signals has the first peak near 2.5 GHz, that corresponds approximately to the wavelength  $\lambda/4=l$ . We are only interested in the amplitudes of the first two Fourier harmonics: for the first one, 402.5 MHz, it is  $A_1 = 0.190$  V, and for the second, 805 MHz,  $A_2 = 0.356$  V.

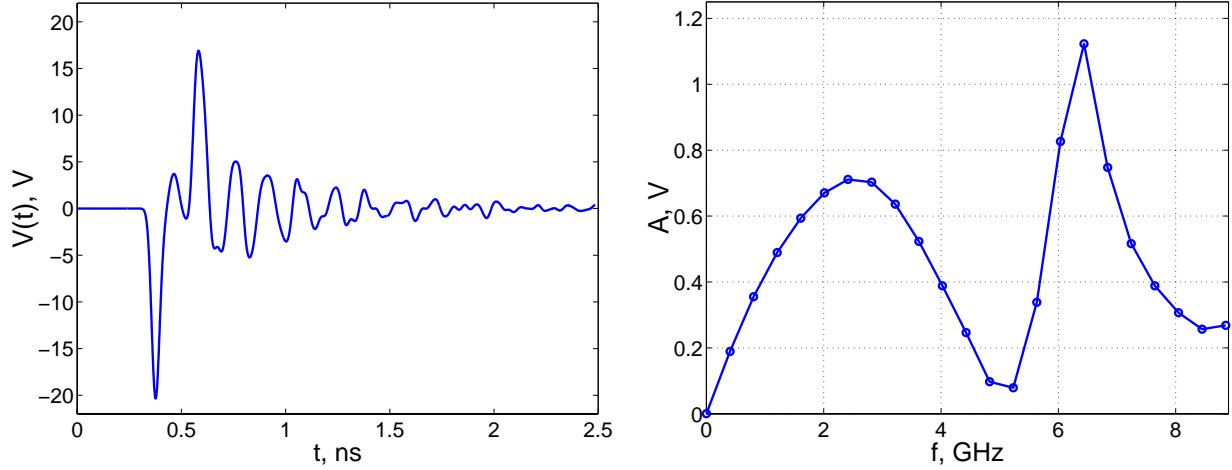


**Figure 4:** Signal on BPM electrodes from a passing on-axis bunch: left – voltage versus time during one period  $T=1/f_b=2.4845$  ns; right – normalized Fourier transform amplitude (V) versus frequency.

Now we extrapolate the MAFIA ultra relativistic results to the H<sup>-</sup> beam energy of 7.5 MeV, i.e. to  $\beta_1=0.126$ , with the following analytical model [3]. For a pencil beam bunch passing the BPM at the transverse position  $x=r\cos\theta$ ,  $y=r\sin\theta$  at velocity  $v=\beta c$ , the signals in the axisymmetric approximation are

$$E(f, r, \theta) = C \frac{\varphi}{2\pi} \left[ \frac{I_0(gr)}{I_0(gr_b)} + \frac{4}{\varphi} \sum_{m=1}^{\infty} \frac{I_m(gr)}{I_m(gr_b)} \sin(m(\phi/2 + \mu)) \cos(m(\theta - \nu)) \right] \quad (1)$$

where  $E=R,T,L,B$  are the Fourier components at frequency  $f$  of the signals on the corresponding electrodes, and the phases  $(\mu, \nu)$  are  $(0,0)$  for  $R$ ,  $(0,\pi/2)$  for  $T$ ,  $(\pi,0)$  for  $L$ ,  $(\pi,\pi/2)$  for  $B$ . Here  $I_m(z)$  are the modified Bessel functions, all dependence on frequency and energy enters through  $g=2\pi f/(\beta\gamma c)$ , and overall coefficient  $C$  depends on the bunch current and shape. The parameters of the model (1) are the BPM effective radius  $r_{\text{eff}}$  and effective subtended angle  $\varphi_{\text{eff}}$ , and they depend only on the geometry of the BPM transverse cross section. The scaling procedure for the model was described in Ref. [1]. It was found that for the cross section under consideration,  $r_{\text{eff}}=1.17r_b$  and  $\varphi_{\text{eff}}=1.24\varphi$  ( $=74.5^\circ$ ), where  $r_b=12.5$  mm,  $\varphi=\pi/3$  rad are the geometrical values. The effective radius  $r_{\text{eff}}=14.625$  mm is close to the average of the electrode inner radius  $r_b=12.5$  mm and that of the BPM enclosure, 17 mm, in agreement with earlier observations [3].

Using MAFIA results for the signal amplitudes, we fix the overall constant  $C$  in Eq. (1) separately for the first and second harmonics. For the first harmonics, at 402.5 MHz,  $C_1=0.918$  V and the ratio  $S(\beta_1)/S(1)=0.80$ ; it results in the beam-induced signal amplitude of **0.152 V** at 7.5 MeV. For the second harmonics, at 805 MHz,  $C_2=1.720$  V and the ratio  $S(\beta_1)/S(1)=0.455$ , that gives the signal amplitude of **0.162 V**. These are the numbers we want to compare with the signals induced by the RF field in the DTL. Figure 5 shows how the signal power changes with the beam velocity for the first two harmonics, according to Eq. (1), for an on-axis bunch as well as for a bunch with a rather large transverse offset.

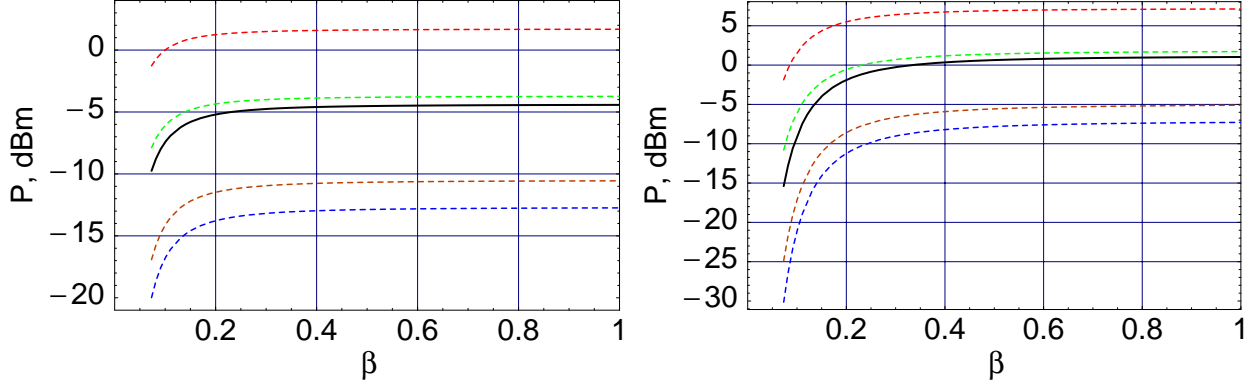


**Figure 5:** Signal power on BPM electrodes from a passing bunch for the 1<sup>st</sup> (left) and 2<sup>nd</sup> Fourier harmonics versus beam velocity, for an on-axis (solid) and a transversely displaced by  $x=r_b/2, y=r_b/4$  beam (4 dashed curves for 4 electrodes).

### **B. RF-induced signal in DTL BPM**

As the next step, we calculate the signal power on the BPM electrodes produced by the 402.5 RF field in the DTL tank. For this purpose, we put the simplified DT of Fig. 3 with the BPM in a cylindrical pillbox having twice the length as the corresponding DTL half-cell, 96 mm, and adjust the pill-box radius to tune its lowest axisymmetric ( $TM_{01}$ -like) mode to the frequency 402.5 MHz. The radius 172 mm gives the required frequency. While this layout is not exactly the same as that in Fig. 1, in particular, in the drift tube details, such a computation gives a good physical picture of how the RF field penetrates into the DT and the BPM, and leads to a reasonable estimate of the induced signal power. The field pattern inside the DT mostly depends on the length and radius of the DT, and the external field frequency. Figure 6 shows the electric field arrows for this mode in the radial cross section near the DT.

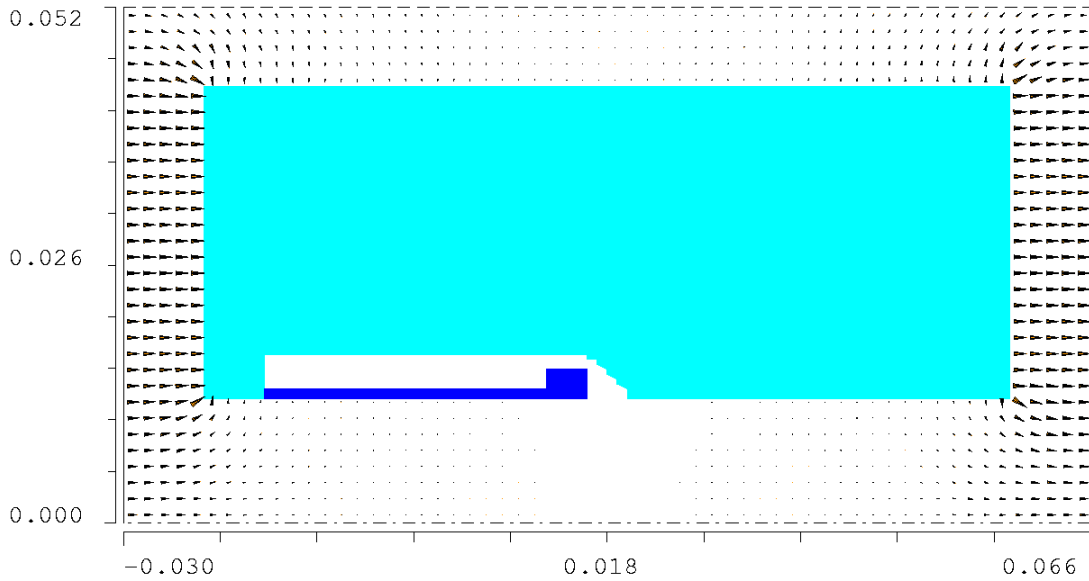


**Figure 6:** Electric field in the partial radial cross section of DT with the BPM inside. The BPM position is shifted to have its gap near the DT center for minimal RF-induced signal. All dimensions are in meters.

To find the amplitude of the voltage induced by the RF field on the BPM electrode connector, we integrate the electric field of the computed 402.5-MHz eigenmode along the connector to get  $V_{\text{con}}$ , and along the beam axis to obtain  $V_{\text{ax}}$ . After that, we calculate the scaling factor from the ratio of the on-axis voltage found by SUPERFISH computations [4],

$$V_{\text{ax-SF}} = 2 \int_{\text{half-cell}} dz E_z = 2.96 \cdot 10^5 \text{ V}$$

to  $V_{\text{ax}}$ . Multiplying  $V_{\text{con}}$  by this scaling factor gives us the RF-induced voltage amplitude  $V_{\text{ind}}$ . The results are listed in Table 1 for a few different positions of the BPM inside the DT. Here  $z_c$  is the longitudinal coordinate of the BPM electrode center relative to the DT middle point, and  $z_g$  is the same for the BPM annular gap center. Recalling that the electrode length is 32 mm, and the gap is 4 mm wide, we have  $z_g - z_c = 32/2 + 4/2 = 18$  mm.

**Table 1:** RF-induced voltage and power on BPM connectors versus BPM position inside DT.

$z_c$ , mm	$z_g$ , mm	$V_{\text{ind}}$ , V	$P$ , dBm
8	24	15.30	33.69
0*	18	3.28	20.32
-8	10	0.72	7.15
-12	6	0.36	1.13
-16	2	0.23	-2.77
-18	0**	0.22	-3.15
-20	-2	0.24	-2.40

\* The electrode center is at the DT center (corresponds to the layout of Fig. 3).

\*\* The gap center is at the DT center (corresponds to the layout of Fig. 6).

It is obvious from Table 1 that placing the BPM gap near the DT center can reduce the RF-induced signal significantly. From physical viewpoint, it is due to the axial symmetry of the RF field: it penetrates effectively only through the BPM annular gap, not through the longitudinal slots between the BPM electrodes.

The important conclusion from the comparison of the RF-induced voltages in Table 1 with the beam-induced voltages in Section 2.A is that they have the same order of magnitude for the optimal BPM position inside the DT: 0.22 V versus 0.15 V at 402.5 MHz, and versus 0.16 V at 805 MHz. While this prevents us from processing BPM signals at 402.5 MHz, we can be sure that (i) this BPM inside the DT can operate with the RF power on without any damage to the cables or electronics, and (ii) the filtering out the 402.5-MHz signal will present no problem for the BPM signal processing at 805 MHz [5].

### ***3. Conclusions***

Electromagnetic modeling of the BPMs for the SNS DTL has been performed with the MAFIA group of codes. Based on the CCL BPM design with four one-end-shortened stripline  $60^\circ$  electrodes [1], the BPM pickup dimensions are adjusted to fit inside the DTs. Time-domain 3D simulations with the SNS bunch are used to calculate the beam induced signals in the BPMs for the ultra relativistic ( $\beta=1$ ) case, and then the results are extrapolated to the lower beam energy with an analytical model in Sect. 2.A. In Sect. 2.B, the RF-induced signals in the BPM inside the drift tube (DT) are calculated using the MAFIA 3D eigensolver, and the BPM position in the DT is optimized to minimize the RF-induced voltages.

The magnitudes of the signal power from the beam and that due to the RF field penetration into the DT are close to each other for the optimized BPM position inside the DT. Therefore, it can be concluded that the DTL BPM can operate with the RF power on, and the 402.5-MHz signals from both the RF and the beam can be filtered out for the BPM signal processing at 805 MHz without problems.

### ***References***

1. S.S. Kurennoy, Tech memos SNS: 99-65, 2000-011; report LA-UR-00-2815.
2. MAFIA Release 4.24, CST GmbH, Darmstadt, 2000.
3. R.E. Shafer, in AIP Conf. Proceed. 319, 1993. – p.303.
4. J.H. Billen, Private communication, June 2000.
5. J.F. Power, Private communication, July 2000.